SELF-ORGANIZED CRITICALITY PARADIGM

I. Ďuran, J. Stöckel, M. Hron, J. Horáček, K. Jakubka, L. Kryška

Institute of Plasma Physics, Association EURATOM/IPP.CR, Acad. Sci. CR,
Za Slovankou 3, PO BOX 17, 182 21 Praha 8, Czech Republic

According to the paradigm of the Self-Organized Criticality (SOC), the anomalous transport in tokamaks is caused by fast transient processes – avalanches. One of the manifestations of these phenomena should be $1/f$ decay of electrostatic fluctuations power spectra in a certain frequency range. In this paper, the frequency spectra of floating potential, density and fluctuation-induced flux, measured by poloidal and radial arrays of Langmuir probes on the CASTOR tokamak, are presented. The floating potential and the fluctuation-induced flux decay from 30 kHz up to 100 kHz as f^{-1}. The plasma density decays as f^{-1} in a more narrow band, 20 – 40 kHz. The possible limitation of SOC behavior for frequencies higher than 100 kHz due to intermittency is stressed. For this reasons the Probability Distribution Functions (PDFs) of floating potential fluctuations were computed at different time scales using wavelet transform. A clear departure of the computed PDFs from Gaussianity, which is a classical signature of intermittency, is observed at time scales under 10 μs (100 kHz).

1   Introduction

The recently formulated paradigm of Self-Organized Criticality (SOC) proposed in [1] is trying to explain experimental observations that are out of the frame of existing theories based on the diffusive nature of transport of particles and heat across magnetic field lines. The concept of SOC assumes appearances of supercritical gradients in tokamak plasmas, which lead to fast transient processes / avalanches. The basic understanding of this model is apparent from comparison with the sand pile, see Fig. 1.
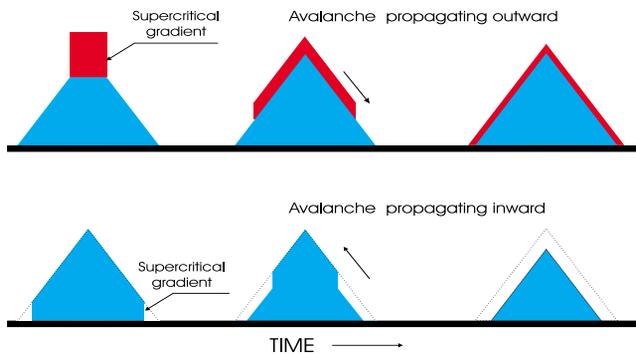

Fig. 1. Sand pile model as a demonstration of Self-Organized Criticality.

The experience of every-day life says that any pile of sand, higher than a critical value, keeps its slope constant independently on its hight. The slope angle is given only by properties of sand grains (material constants). The pile of sand is in critical state. Adding a shovel of sand on the top of such critical pile results in creation of a super critical gradient (higher than critical slope). This causes an "avalanche" of sand propagating downwards that restores the original critical state. This process is demonstrated in the upper sequence of Fig. 1. The lower sequence displays also possibility of avalanche propagating uphill. Removal of some sand at the sand pile edge causes again super critical gradient and consequently collapse that can be seen as an avalanche propagating toward the center of the pile leaving it in the critical state in the end. In tokamaks, the critical slope is represented by equilibrium gradients of density, temperature, pressure, etc. Any sudden influx or outflux of heat or particles can lead to super-critical gradient within the plasma volume and consequently to avalanches and increased transport.

One of the manifestations of this phenomena in tokamak plasma should be f^{-1} decay of electrostatic fluctuations power spectra in the certain frequency range as presented in [3]. Possible limitations of SOC paradigm validity for RFX plasma due to intermittency are presented in [2].

Experiments are carried on CASTOR tokamak ($R = 40$ cm, $a = 8.5$ cm) at $B_T = 1$ T, $I_p = 8 \div 13$ kA and average densities $\bar{n}_e = 0.5 \div 1.5 \cdot 10^{19} \mathrm{m}^{-3}$ to test and extend results mentioned in refs. [2] and [3] for small tokamak plasmas.

The fluctuations are monitored by using a poloidal and radial arrays of 16 Langmuir probes (LPs) with spatial resolution 2.5 mm (for more details see [4]), inserted into the plasma from the top of the torus. Individual tips measure either the floating potential U_{fl} or the ion saturation current I_{sat}. Each array is fixed on a radially movable arm. The sampling frequency of A/D converters was up to 1 MHz.

2 Results

2.1 Spectral properties

Following set of figures (Fig. 2) demonstrates spectral properties of plasma edge electrostatic turbulence in the proximity of magnetic surface where the poloidal plasma rotation changes its sign – Velocity Shear Layer (VSL). Position of VSL is identified with radius where U_{fl} reaches its maximum value.

The three figures in the left column show the U_{fl} power spectra at three different radial positions. The top spectrum was measured 5 mm inside VSL, the middle one roughly at VSL and the bottom one 5 mm outside VSL. All the spectra in this column are averaged over 30 shots with similar plasma parameters. The three distinct spectral ranges are well pronounced in all the three figures: 0 – 11 kHz (corresponding to coherent modes), 11 – 50 kHz (SOC relevant region), and over 50 kHz (microturbulence). However, only in the middle figure (measured at VSL) the spectrum decays as $f^{-0.8}$ in the frequency range 11 – 50 kHz almost as predicted
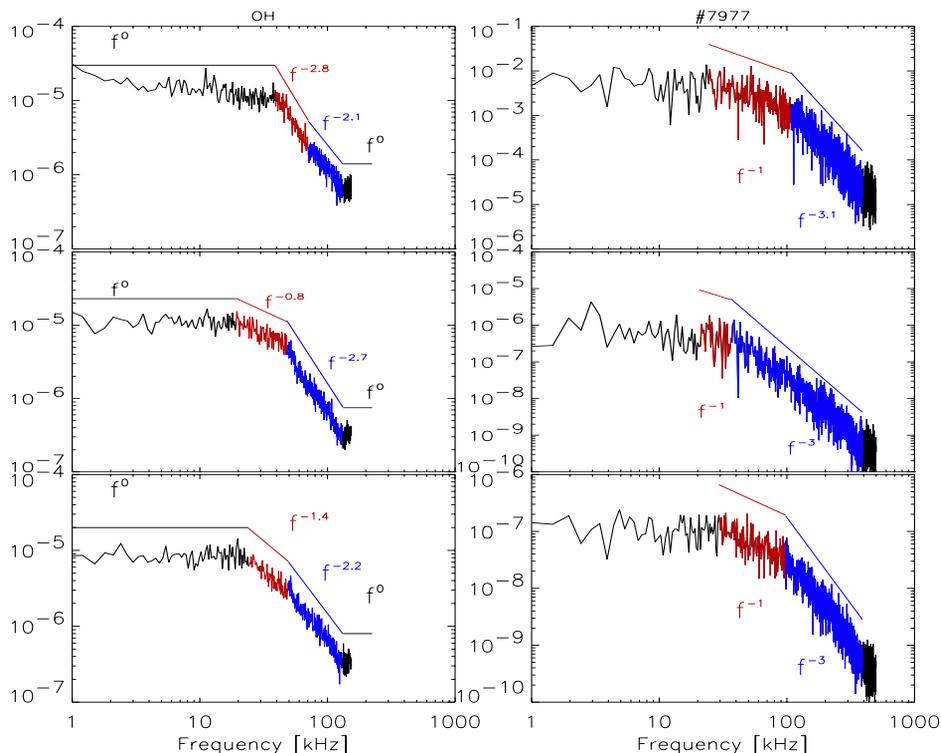
Fig. 2. Left column: Power spectra of U_{fl} fluctuations: top - 5 mm inside VSL, middle - at VSL and bottom - 5 mm outside VSL, measured by radial array of LPs. Right column: Power spectra (from top to bottom) of E_θ, I_{sat} *and* Γ all at VSL, measured by poloidal array of LPs.

by SOC theory ($1/f$ decay is predicted). Because of poloidal plasma rotation, which is zero only at VSL, the top and the bottom spectrum is misshapen by Doppler shift. This could be a reason, why different power law is observed in these cases. The three figures in the right column are, from top to bottom, the power spectra of poloidal electric field E_θ, ion saturation current ($\sim$ density) I_{sat} and, fluctuations-induced flux Γ all measured at VSL (no poloidal plasma rotation – checked by the correlation analysis of poloidal LPs data) by poloidal array of LPs in a single shot. Again, the three spectral bands with a power law decay are clearly identified for all three quantities. The results are summarized in the following Table 1: After more precise suppression of Doppler shift in this case, the $1/f$ decay is observed for E_θ and Γ in the range $\sim$ 30 kHz – 100 kHz, while for I_{sat} the band is more narrow 20 kHz – 40 kHz. These results support relevance of SOC theory for the CASTOR plasma.

Table 1.

	E_θ	I_{sat}	Γ
f^0 [kHz]	0÷20	0÷20	0÷30
f^{-1} [kHz]	20÷100	20÷40	30÷100
f^{-3} [kHz]	100÷400	40÷400	100÷400

2.2 PDFs of electrostatic turbulence

Already the spectral analysis suggests that there are limitations of SOC as a significant transport mechanism in tokamaks ($1/f$ decay only in the frequency band ~ 10 – 100 kHz). One of the basic assumptions in SOC theory is that considered processes are self-similar, that means, they have the same statistical properties at different time scales. Validity of this assumption for CASTOR turbulence data was tested using wavelet analysis. The computed Probability Distribution Functions (PDFs) and their fits by Gaussian distribution at different time scales are displayed in the Fig. 3. A clear departure of PDFs wings from Gaussian distribution for scales under
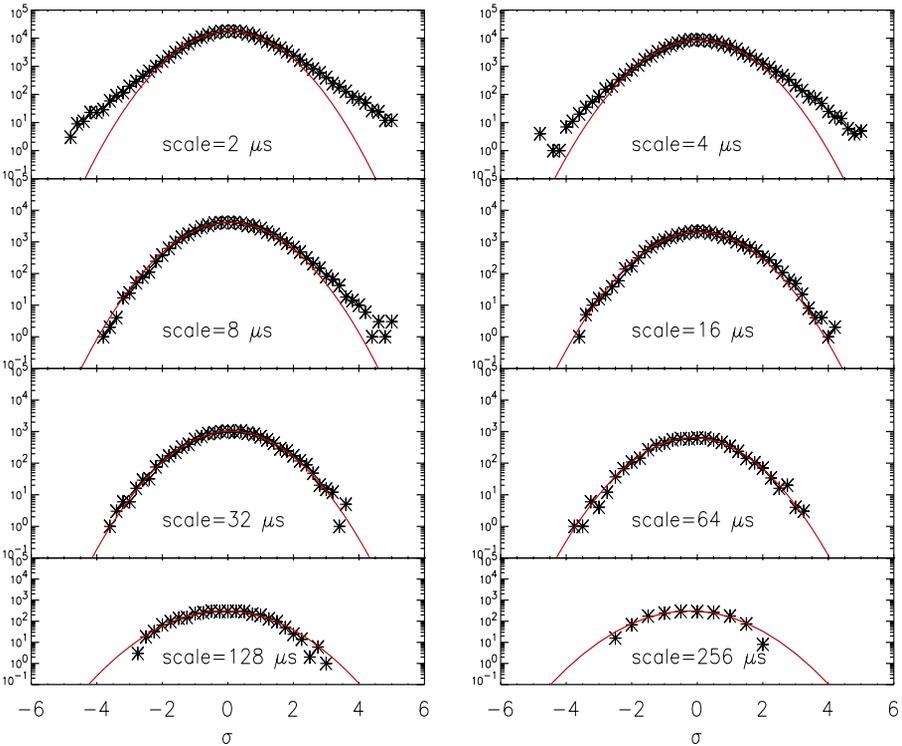

Fig. 3. PDFs of U_{float} at different time scales averaged over 24 shots and different radial positions at the plasma edge and scrape of layer. Full line denotes Gaussian fit.

$\sim 10\ \mu$s (for frequencies above 100 kHz) is observed. This enhancement is a typical signature of self-similarity break-down called intermittency. The similar results were obtained also at RFX [2].

3   Conclusions

Edge electrostatic fluctuations are analyzed using Fourier and Wavelet analysis to study relevance of SOC model for CASTOR edge plasmas. Three well pronounced frequency bands with a different power law decay are typically observed for frequency power spectra of electrostatic turbulence. $1/f$ decay is observed in frequency band $\sim 10 - 100$ kHz at VSL (no poloidal plasma rotation). This supports the relevance of SOC induced transport for CASTOR plasmas. Possible limitations of SOC behavior importance for microturbulence (above 100 kHz) due to intermittency is pointed out.

References

[1] P. Bak et al.: Phys. Rev. Lett. **59** (1987) 381.

[2] V. Carbone et al.: Physics of Plasmas **7**(2) (2000) 445.

[3] P. Beyer et al.: Plasma Physics and Controlled Fusion **41** (1999) A757.

[4] J. Stöckel et al.: Plasma Physics and Controlled Fusion **41** (1999) A577.